

# The entanglement entropy and the Berry phase in solid states

S. Ryu

*Kavli Institute for Theoretical Physics, University of California, Santa Barbara, CA 93106, USA*

Y. Hatsugai

*Department of Applied Physics, University of Tokyo, Hongo Bunkyo-ku, Tokyo 113-8656, Japan*

(Dated: December 2, 2024)

The entanglement entropy (von-Neumann entropy) has been used to characterize the quantum entanglement of many-body ground states in strongly correlated systems. In this paper, we try to establish a connection between the lower bound of the von-Neumann entropy and the Berry phase defined for quantum ground states. As an example, a family of one-dimensional (1D) Hamiltonians with two bands separated by a finite gap is investigated. We argue that when the Berry phase (Zak's phase) of the occupied band is equal to  $\pm\pi \times (\text{odd integer})$  and when the ground state respects a discrete unitary particle-hole symmetry (chiral symmetry), the entanglement entropy in the thermodynamic limit is at least larger than  $\ln 2$  (per boundary), i.e., the entanglement entropy that corresponds to a maximally entangled pair of two spins. We also discuss the lower bound is related to vanishing of the expectation value of a certain non-local operator which creates a kink in 1D systems.

## I. INTRODUCTION

A distinctive feature of ground states in quantum phases of matter is that they can be highly entangled and thus exhibit essentially different features from classical systems. For example, they are not completely characterized by vanishing or non-vanishing of order parameters of some kind, which is in a sharp contrast to classical statistical systems. Instead, quantum ground states should be described by their pattern of entanglement such as topological or quantum order. [1] However, beyond some simple textbook examples such as a system of two coupled  $S = 1/2$  spins (qubits), we do not have many intuitions about entanglement properties hidden in many-body wave functions. The entropy of entanglement (von-Neumann entropy) [2]

$$S_A = -\text{tr}_A \rho_A \ln \rho_A, \quad \rho_A = \text{tr}_B |\Psi\rangle\langle\Psi|, \quad (1.1)$$

can provide us a convenient way to measure how closely entangled (or how "quantum") a given ground state wave function  $|\Psi\rangle$  is. Here, the total system is divided into two subsystems  $A$  and  $B$  and  $\rho_A$  is the reduced density matrix for the subsystem  $A$  obtained by taking a partial trace over the subsystem  $B$  of the total density matrix  $\rho = |\Psi\rangle\langle\Psi|$ . This quantity is zero for classical product states whereas it takes a non-trivial value for valence-bond solid states (VBS), or resonating valence bond states (RVB), say. Recently, the entanglement entropy at and close to quantum phase transitions in low-dimensional strongly correlated systems has been used as a new tool to investigate the nature of quantum criticality. [3, 4, 5, 6, 7, 8, 9] Even though the entire phase of one-dimensional (1D) quantum systems can be well described by their entanglement properties, it is not always clear what different information other than that contained in conventional correlation functions is actually carried by the von-Neumann entropy.

On the other hand, the Berry phase [10] associated with (many-body) wave functions in solid states has been used to detect quantum mechanical phase degrees of freedom. Probably, it is best epitomized by the Thouless-Kohmoto-Nightingale-Nijs (TKNN) formula in the integer quantum Hall effect (IQHE) [11, 12], in which gapped quantum phases are distinguished by an integral topological invariant originating from winding of the phase of wave functions. In addition to the IQHE, the Berry phase also appears in the King-Smith-Vanderbilt (KSV) formula [14, 15] of the theory of macroscopic polarization, and its incarnation in quantum spin chains [16, 17], and so on. An observable consequence of the non-trivial Berry phase is the existence of localized states at the boundaries when we terminate a system with boundaries. [18, 19, 20]

It is then tempting to ask if there is, if any, a connection between these two paradigms in quantum physics, namely, entanglement and the Berry phase, which is our main focus in the present work. We mainly consider gapped quantum phases for which the Berry phase is well-defined, a point of view which is complementary to a flurry of recent works focusing on quantum critical points.

With some specific examples, we will demonstrate that taking the partial trace over a subsystem corresponds to creating boundaries in a system. Two contributions to the entanglement entropy will be then identified. The first one is of type already discussed in the context of 1D many-body systems which obeys, when we are at a critical point, a logarithmic behavior  $S_A \sim \frac{c}{3} \ln L$  where  $c$  is the central charge of the conformal field theory that governs the criticality, and  $L$  the size of the subsystem  $A$ . [8] The other comes from the localized boundary states which are protected by topology of the band structure and symmetries of some sorts as discussed in Refs. [18, 19]. The former contribution is related to the real part of the logarithm of the expectation value of the

twist operator, which can be expressed by the quantum metric[21], whereas the latter to its imaginary part and to the Berry phase. [See Eqs. (2.4) to (2.7).] We thus clarify information of quantum many-body wavefunctions included in the von-Neumann entropy is connected to the Berry phase. Furthermore, this implies that we can make use of our previous knowledge on edge states [18, 19, 20] to obtain the lower bound of the entanglement entropy.

We also discuss that the lower bound of the von-Neumann entropy is related to vanishing of the expectation value of a certain non-local operator which creates a kink in 1D systems.

## II. 1D TWO-BAND SYSTEMS

In order to explore a connection between the Berry phase (Zak's phase) and the entanglement entropy in solid states, it would be good to start from 1D translational invariant systems with two bands separated by a finite gap, which is the simplest situation we can think of:

$$\mathcal{H} = \sum_{x,x'}^{\text{PBC}} \mathbf{c}_x^\dagger H_{x-x'} \mathbf{c}_{x'}, \quad H_{x-x'} = \begin{pmatrix} t_+ & \Delta \\ \Delta' & t_- \end{pmatrix}_{x-x'}. \quad (2.1)$$

Here, a pair of fermion annihilation operators  $\mathbf{c}_x^T = (c_+, c_-)_x$  is assigned for each site,  $x, x' = 1, \dots, N$ , and the hermiticity of  $\mathcal{H}$  implies  $t_{\iota, x-x'} = t_{\iota, x'-x}^*$  and  $\Delta_{x-x'} = (\Delta'_{x'-x})^*$  for  $\iota = \pm$ . In spite of its simplicity, this Hamiltonian (2.1) has a wide range of applicability, such as superconductivity, graphite systems [18], ferroelectricity of organic materials and perovskite oxides [22], and the slave boson mean field theory for spin liquid states, say. By the Fourier transformation  $\mathbf{c}_x = N^{-1/2} \sum_{k \in \text{Bz}} e^{ikx} \mathbf{c}_k$ , with  $k = 2\pi n/N$  the Hamiltonian in the momentum space is given by  $\mathcal{H} = \sum_{k \in \text{Bz}} \mathbf{c}_k^\dagger H(k) \mathbf{c}_k$ , where  $H(k) := \sum_x e^{-ikx} H(x)$ . If we introduce an “off-shell” four-vector  $R^{\mu=0,1,2,3}(k) \in \mathbb{R}$  by  $R^0(k) \mp R^3(k) := t_{\pm}(k)$ ,  $-R^1(k) + iR^2(k) := \Delta(k)$ , we can rewrite the Hamiltonian in the momentum space as

$$\mathcal{H} = \sum_{k \in \text{Bz}} \mathbf{c}_k^\dagger R^\mu(k) \sigma_\mu \mathbf{c}_k, \quad (2.2)$$

where  $\sigma_\mu = (\sigma_0, -\boldsymbol{\sigma})$  with  $\sigma_0 = \mathbb{I}_2$ .

Observing that  $R^\mu \sigma_\mu$  is diagonalized by the same eigen vectors as those of  $R_i \sigma_i = \mathbf{R} \cdot \boldsymbol{\sigma}$  (but with different eigenvalues), normalized eigenstates  $\vec{v}_\pm$  for  $R^\mu \sigma_\mu$  are given by, when  $\mathbf{R}$  is not in the Dirac string,  $(R^1, R^2) \neq (0, 0)$ , [10]

$$\vec{v}_\pm = \frac{1}{\sqrt{2R(R \mp R^3)}} \begin{pmatrix} R^1 - iR^2 \\ \pm R - R^3 \end{pmatrix}, \quad (2.3)$$

where  $R = |\mathbf{R}|$  (should not be confused with  $R^0$ ), and the eigenvalue for  $\vec{v}_\pm$  is  $E_\pm = R^0 \mp R$ . The Hamiltonian is then diagonalized as  $\mathcal{H} = \sum_k \boldsymbol{\alpha}_k^\dagger \text{diag}(E_+, E_-)_k \boldsymbol{\alpha}_k$ , where  $c_{\iota, k} = (\vec{v}_\sigma)^\iota \alpha_{\sigma, k}$ . As we assume there is a finite gap

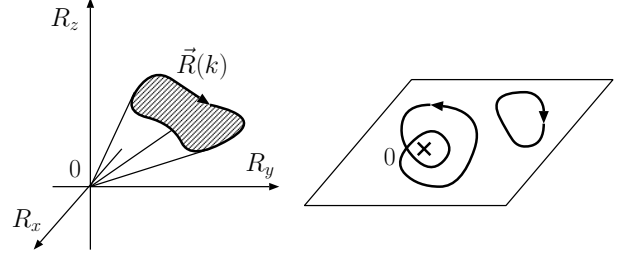


FIG. 1: (Left) The loop defined by  $\mathbf{R}(k)$  in  $\mathbf{R}$ -space. (Right) Loops for chiral symmetric Hamiltonians.

for the entire Brillouin zone,  $E_+ > E_-$ ,  $\forall k \in \text{Bz}$ . The vacuum  $|\Psi\rangle$  is the filled Fermi sea  $|\Psi\rangle = \prod_{k \in \text{Bz}} \alpha_{-,k}^\dagger |0\rangle$ .

The Berry phase can be defined through the expectation value of the twist operator:

$$z := \exp \left[ i \frac{2\pi}{N} \sum_x x n_x \right], \quad (2.4)$$

where  $n_x$  is the electron number operator at site  $x$ ,  $n_x = \sum_\iota c_{x,\iota}^\dagger c_{x,\iota}$ . For the Fermi-sea  $|\Psi\rangle$ , the expectation value of the twist operator is calculated as

$$\langle \Psi | z | \Psi \rangle = (-1)^{N+1} \exp [i\gamma - \xi^2/N + \mathcal{O}(1/N^2)], \quad (2.5)$$

where the Berry phase (Zak's phase)  $\gamma$  is given by a line integral of the gauge field  $A(k)$  over the 1D Brillouin zone (Bz) [13, 14, 15, 23],

$$\begin{aligned} iA_x(k) &:= \langle v_-(k) | \frac{d}{dk} | v_-(k) \rangle, \\ \gamma &:= i \int_0^{2\pi} iA_x(k) dk. \end{aligned} \quad (2.6)$$

For the Fermi-sea  $|\Psi\rangle$  derived from the Hamiltonian (2.2),  $\gamma$  is simply equal to half of the solid angle sustained by a loop defined by  $\mathbf{R}(k)$  in  $\mathbf{R}$ -space [10, 18]. (Fig. 1) On the other hand, the  $\mathcal{O}(1/N)$  correction to  $\ln \langle \Psi | z | \Psi \rangle$  is real and given by the integral of the quantum metric  $g_{xx}(k)$  over the Bz [21],

$$\begin{aligned} g_{xx}(k) &:= \text{Re} \langle \partial_k v_- | \partial_k v_- \rangle - \langle \partial_k v_- | v_- \rangle \langle v_- | \partial_k v_- \rangle, \\ \xi^2 &:= \pi \int_0^{2\pi} g_{xx}(k) dk. \end{aligned} \quad (2.7)$$

It is known that  $\xi^2$  is related to the correlation length.

### A. the truncated correlation matrix and its zero modes

We next partition the system into two parts,  $A = \{x | x = 1, \dots, N_A\}$  and  $B = \{x | x = N_A + 1, \dots, N_B\}$  with  $N_A + N_B = N$ , and ask, with the von-Neumann entropy  $S_A$ , to what extent these two subsystems are entangled. Instead of directly tracing out the subsystem

$B$  following the definition (1.1), we can make use of correlation matrix  $C_{\iota\lambda}(x-y) := \langle c_{(x,\iota)}^\dagger c_{(y,\lambda)} \rangle$  as shown in Ref. [24]. From the entire correlation matrix, we extract the submatrix  $\{C_{\iota\lambda}(x-y)\}_{x,y \in A}$  where  $x, y$  is restricted in the subsystem  $A$ . The entanglement entropy is then given by

$$S_A = - \sum_a \left[ \zeta_a \ln \zeta_a + (1 - \zeta_a) \ln(1 - \zeta_a) \right], \quad (2.8)$$

where  $\zeta_a$  are the eigenvalues of the truncated correlation matrix  $\{C_{\iota\lambda}(x-y)\}_{x,y \in A}$ .

With the whole set of the eigen values and eigen wavefunctions in hand, the correlation matrix  $C_{\iota\lambda}(x-y) = N^{-1} \sum_{k \in Bz} e^{-ik(x-y)} C_{\iota\lambda}(k)$  is calculated exactly as

$$C_{\iota\lambda}(k) = \frac{1}{2} [n^\mu(k) \sigma_\mu]_{\iota\lambda}, \quad (2.9)$$

where we have introduced an “on-shell” four-vector  $n^\mu$  by  $n^\mu = (1, \mathbf{R}/R)$ . It should be noted that a set of Hamiltonian share the same ground state wavefunction and thus the same correlation matrix.

The basic idea we will use to discuss the entanglement entropy is to think that the correlation matrix  $C(x-y)$  defines a 1D “Hamiltonian” with PBC. This “Hamiltonian” (let us call it the correlation matrix Hamiltonian or the  $\mathcal{C}$ -Hamiltonian for simplicity) has the same set of eigen wave functions as the original Hamiltonian but all the eigenvalues are given by either 1 or 0. The range of hopping elements in the generated system is order of the inverse gap of the original Hamiltonian. I.e., if there is a finite gap, the  $\mathcal{C}$ -Hamiltonian is local (short-ranged).

Now, what we need to know is what energy spectrum the  $\mathcal{C}$ -Hamiltonian will have when we cut it into two parts, defined by  $A$  and  $B$ . This is the same question asked in Ref. 18, in which a criterion to determine the existence of zero-energy edge states is presented. There are two types of eigen values in the energy spectrum of the truncated  $\mathcal{C}$ -Hamiltonian in the thermodynamic limit  $N_A \rightarrow \infty$ . Eigenvalues of the first type are identical to their counterpart in the periodic (untruncated) system. On top of it, there appear localized boundary states whose eigenvalues are located within the bulk energy gap. Since the eigenvalues that belong to the bulk part of the spectrum are either 1 or 0, they do not contribute to the entanglement entropy whereas the boundary modes do.

The question is then how many boundary states appear and with what energy when the system is truncated. As suggested from the the KSV formula in macroscopic polarization, the non-vanishing Berry phase of the filled band of the  $\mathcal{C}$ -Hamiltonian implies the existence of states localized near the boundary. Remembering the original and generated Hamiltonians share the same set of eigen wave functions, the Berry phase for the generated system is identical to that of the original system.

If we impose a discrete symmetry implemented by a unitary particle-hole transformation, so-called chiral symmetry, on the  $\mathcal{C}$ -Hamiltonian, it is possible to make

a precise prediction for the number of boundary states that has an eigen value  $\zeta = 1/2$ , following the same line of discussion in Ref. 18. When the system respects the chiral symmetry, we can find a unitary matrix that anti-commutes with the one-particle Hamiltonian. For this case,  $\mathbf{n}(k)$  is restricted to lie on a plane cutting the origin in  $\mathbf{R}$ -space, which in turn means that the Berry phase for the lower band of  $\mathcal{H}$  is equal to  $n\pi$  ( $n \in \mathbb{N}$ ). (Fig. 1) When  $n$  is odd, we can show that there are at least a pair of boundary modes at  $\zeta = 1/2$ , one of which is localized at the left end and the other at the right. [25] (The system with  $\gamma = \pm\pi$  is, in a sense, “dual” to that with the vanishing Berry phase where there is no boundary state. See Appendix.) Then, the lower bound of the entanglement entropy is given by

$$S_A \geq -\ln \frac{1}{2} - \ln \frac{1}{2} = 2 \ln 2. \quad (2.10)$$

This lower bound is equal to the entanglement entropy contained in a dimer for each end of the original model, which is consistent with the fact that the origin of the boundary states discussed above can be traced back to dimers in the reference Hamiltonian to which a given target Hamiltonian is adiabatically connected.

There can be other contributions from boundary states that are not connected to a dimer in the above sense. Indeed, as we will explicitly demonstrate below, this kind of boundary modes proliferate as we approach a quantum critical point whose number grows as  $\sim \frac{1}{6} \ln \frac{1}{m}$  where  $m$  is the gap, and finally gives rise to the logarithmic divergences at the critical point. [8] Note also that our discussion here does not apply gapless systems since the matrix elements of the  $\mathcal{C}$ -Hamiltonian are long-ranged in this case.

## B. example 1; the dimerized Hamiltonians

As a simple example of a two-band Hamiltonian and the correlation matrix, let us consider the case in which the correlation matrix is given by a four vector  $n^\mu$  with

$$\mathbf{R}(k) = (-\Delta \cos k, -\Delta \sin k, \xi), \quad (2.11)$$

where  $\Delta, \xi \in \mathbb{R}$ . There is a family of Hamiltonians having this correlation matrix which includes the “dimerized” Hamiltonian,  $\mathcal{H} = \sum_x \left[ \sum_\iota \iota \xi c_{x\iota}^\dagger c_{x\iota} + \Delta c_{x+1,+}^\dagger c_{x,-} + \text{h.c.} \right]$ . The inverse Fourier transformation gives the correlation matrix in the tight-binding notation,  $\mathcal{C} = (2R)^{-1} \sum_x \left[ \sum_\iota (R - \iota \xi) c_{x\iota}^\dagger c_{x\iota} - \Delta c_{x+1,+}^\dagger c_{x,-} + \text{h.c.} \right]$ . This  $\mathcal{C}$ -Hamiltonian can be diagonalized for both periodic and truncated boundary conditions by introducing the “dimer” operators via  $d_{\pm, x+\frac{1}{2}}^\dagger = (c_{x,+}^\dagger \pm c_{x+1,-}^\dagger)/\sqrt{2}$ . (See also Appendix.) The truncated  $\mathcal{C}$ -Hamiltonian has  $(N-1)$ -fold degenerate eigenvalues  $\zeta = 0, 1$ , and two eigenvalues  $\zeta = (1 \pm \frac{\xi}{R})/2$  that correspond to edge states.

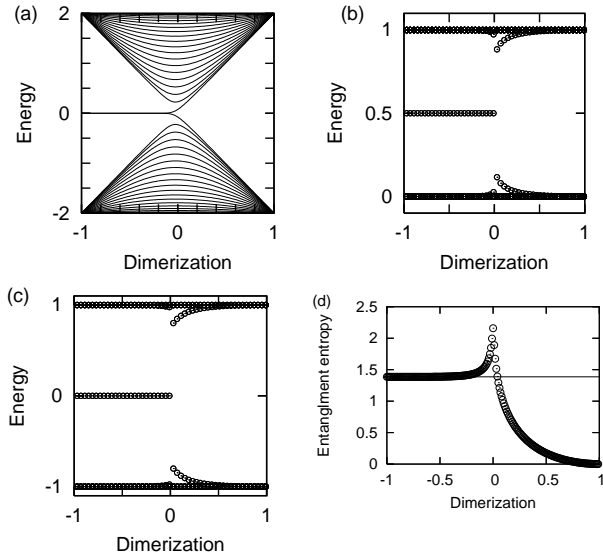


FIG. 2: The energy spectra of (a) the Hamiltonian  $\mathcal{H}$  with open ends, (b) the truncated correlation matrix  $\mathcal{C}$ , and (c) the matrix  $\mathcal{S}$  as a function of the dimerization parameter  $\phi \in [-1, 1]$  for the SSH model. (d) The entanglement entropy of the SSH model.

The entanglement entropy (in the thermodynamic limit) is then computed as

$$\frac{1}{2}S_A = -\frac{\gamma}{2\pi} \ln \frac{\gamma}{2\pi} - \frac{(2\pi - \gamma)}{2\pi} \ln \frac{2\pi - \gamma}{2\pi}. \quad (2.12)$$

where the Berry phase  $\gamma$  for the correlation matrix (2.11) is  $\gamma/\pi = 1 - \xi/R$ . In the two extreme cases, we have  $\xi = 0$  and  $\xi \rightarrow \pm\infty$ ,  $S_A(\xi = 0) = 2 \ln 2$  and  $S_A(\xi \rightarrow \pm\infty) = 0$ . The entanglement entropy in the present case is a convex function with respect to  $\gamma \in [0, 2\pi]$  and the maximum is achieved when  $\gamma = \pi$  whereas two minima are located at  $\gamma = 0, 2\pi$ .

### C. example 2: the Su-Schrieffer-Heeger model

As a next example, let us look at a situation in which two phases with the Berry phase  $\gamma = \pi$  and 0 are connected by a quantum phase transition point. Physically, such an example is provided by the Su-Schrieffer-Heeger (SSH) model for a chain of polyacetylene. The 1D tight-binding Hamiltonian for the SSH model for a chain of polyacetylene is given by  $\mathcal{H} = \sum_{i=1}^{N_i} t(-1 + (-1)^i \phi_i)(c_i^\dagger c_{i+1} + \text{h.c.})$  [26] where  $\phi_i$  represents dimerization at the  $i$ -th site, and an alternating sign of the hopping elements reflects dimerization between the carbon atoms in the molecule. Here, we treat the lattice in a classical fashion and neglected its elastic (kinetic) energy. Taking  $\phi_i = \phi = \text{const.}$ ,  $t = 1$ , and defining a spinor at  $x = 2i - 1$  by  $\mathbf{c}_x = (c_i, c_{i+1})^\text{T}$ , the Hamiltonian can be

written as ( $N = N_i/2$ )

$$\mathcal{H} = \sum_{x=1}^N \mathbf{c}_x^\dagger \begin{pmatrix} -(1+\phi) & 0 \\ -(1-\phi) & 1-\phi \end{pmatrix} \mathbf{c}_x - \mathbf{c}_x^\dagger \begin{pmatrix} 0 & 1-\phi \\ 1-\phi & 0 \end{pmatrix} \mathbf{c}_{x+1} + \text{h.c.} \quad (2.13)$$

Under the PBC, the SSH Hamiltonian can be diagonalized as Eq. (2.2) with  $R_x(k) = -1 - \phi - (1 - \phi) \cos k$ ,  $R_y(k) = (-1 + \phi) \sin k$ ,  $R_z(k) = 0$ .

For  $\phi \in [-1, 0)$ , the Berry phase is given by  $\gamma = \pi$  whereas for  $\phi \in (0, 1]$   $\gamma = 0$ . These two phases are separated by a quantum phase transition at  $\phi = 0$ . Following the discussion in Ref. [18], there is at least pair of boundary states for  $\phi \in [-1, 0)$  when we terminated the system. Indeed, for the numerically computed energy spectrum of the SSH model with open ends (Fig. 2) for  $\phi \in [-1, +1]$ , there is a pair of edge states for  $\forall \phi \in [-1, 0)$ .

The entanglement entropy is calculated by diagonalizing the  $\mathcal{C}$ -Hamiltonian. The energy spectrum of the  $\mathcal{C}$ -Hamiltonian with open ends is shown in Fig. 2. Again, there is a pair of boundary states for  $\phi \in [-1, 0)$  and for this case,  $S_A$  is bounded from below as  $S_A \geq 2 \ln 2$ . (Fig. 2) When we approach the transition point  $\phi = 0$ , some bulk eigenvalues turn into the boundary eigenvalues and they give rise to extra contributions other than the zero-energy boundary states. Similar behavior of the entanglement entropy is discussed for the quantum Ising chain in transverse magnetic field, where the  $2 \ln 2$  entropy originates from a Schrödinger cat state composed of all spin up and down configurations.

### III. CONNECTION TO A KINK OPERATOR

We have seen that bipartitioning the system corresponds to an introduction of a sharp ‘‘boundary’’ (interface). In this section, we will realize it by a non-local operator, a kink operator

$$\eta := \exp \left[ i \sum_x \varphi(x) n_x \right], \quad \eta^\dagger = \eta, \quad (3.1)$$

where

$$\varphi(x) := \begin{cases} 0, & x \in A, \\ \pi, & x \in B. \end{cases} \quad (3.2)$$

The geometric mean of this kink operator is the twist operator. [27]

The kink operator attaches a phase factor  $\varphi(x)$  for the fermion operators at cite  $x$ ,

$$\eta^\dagger c_{xt} \eta = e^{+i\varphi(x)} c_{xt}, \quad \eta^\dagger c_{xt}^\dagger \eta = e^{-i\varphi(x)} c_{xt}^\dagger. \quad (3.3)$$

Thus, if we introduce the reduced density operator through

$$\tilde{\rho}_A := \frac{1}{2} [\eta |\Psi\rangle \langle \Psi| \eta^\dagger + |\Psi\rangle \langle \Psi|], \quad (3.4)$$

the matrix elements  $\text{tr} [c_{x,\iota}^\dagger c_{y,\lambda} \tilde{\rho}_A]$  are vanishing whenever  $x \in A$  and  $y \in B$  and vice versa, whereas they coincide with the correlation matrix  $C_{\iota\lambda}(x-y)$  when  $x, y \in A$ . Unlike  $\rho_A$ , the matrix elements  $\text{tr} [c_{x,\iota}^\dagger c_{y,\lambda} \tilde{\rho}_A]$  are non-zero even for the  $B$  subsystem. This “padding” does nothing however.

In the following, we will discuss the expectation value of the kink operator  $\langle \Psi | \eta | \Psi \rangle$  with respect to a given ground state wave function  $|\Psi\rangle$  which is related to the expectation value of  $\tilde{\rho}_A$  as  $\langle \Psi | \tilde{\rho}_A | \Psi \rangle = \frac{1}{2} [\langle \Psi | \eta | \Psi \rangle^2 + 1]$ . As we will see the vanishing of  $\langle \Psi | \eta | \Psi \rangle$  is closely related to a  $\ln 2$  contribution to  $S_A$  discussed in the previous section. This can be understood intuitively as follows. Classical wave functions can be written as a product state and are rather insensitive to the kink operator. Thus, the ground state with the kink operator inserted  $\eta|\Psi\rangle$  has a large overlap with the original ground state  $|\Psi\rangle$ . On the other hand, the kink operator destroys dimers if the Berry phase of the ground state is  $\pi \times$  (odd integer). As a consequence the overlap  $\langle \Psi | \eta | \Psi \rangle$  is very small in this quantum phase, which in turn suggests that quasi-particles that constitute the continuum spectrum above the ground state can be interpreted as a kink created by  $\eta$ . Thus the kink operator is capable of distinguishing the quantum phases with different entanglement properties.

To put the above statement in a quantum information perspective, remember the reduced density matrix  $\tilde{\rho}_A$  is in general in a mixed state:

$$\tilde{\rho}_A = \sum_n p_n |\Psi_n \otimes 0\rangle \langle \Psi_n \otimes 0|, \quad (3.5)$$

where  $|\Psi_n\rangle$  belongs to the subsystem  $A$ , and  $\sum_n p_n = 1$ . When the wavefunction  $|\Psi\rangle$  happens to be a completely entanglement-free, product state,  $|\Psi\rangle = |\Psi_A\rangle \otimes |\Psi_B\rangle$ , the reduced density matrix  $\tilde{\rho}_A$  is in a pure state, i.e.,  $p_{n\neq 1} = 0$ ,  $p_n = 1$ ,  $|\Psi_1\rangle = |\Psi_A\rangle$ . On the other hand, when  $|\Psi\rangle$  is highly entangled, taking partial trace over the  $B$  subsystem generates many pure states  $|\Psi_n\rangle$  with non-zero weight  $0 < p_n < 1$ . How far a given state  $|\Psi_n\rangle$  from a product state can then be measured by taking the expectation value of the reduced density matrix  $\tilde{\rho}_A$ :

$$\langle \Psi | \tilde{\rho}_A | \Psi \rangle = \sum_n p_n \langle \Psi | \Psi_n \otimes 0 \rangle \langle \Psi_n \otimes 0 | \Psi \rangle. \quad (3.6)$$

Clearly, it is equal to one when  $|\Psi_n\rangle$  is a product state whereas it is expected to be less than one for entangled states.

In the following subsections, we will establish that in an insulating phase the expectation value of the kink operator is zero in the thermodynamic limit when the Berry phase is  $\pi \times$  odd integer whereas it is finite otherwise.

### A. the expectation value of the kink operator as a determinant

The computation of the expectation value of the kink operator for a Fermi-Dirac sea  $|\Psi\rangle = \prod_{k \in \text{Bz}} \alpha_{-,k}^\dagger |0\rangle$  goes

as follows. In the momentum space, the phase attachment transformation (3.3) reads

$$\eta^\dagger \mathbf{c}_k \eta = \sum_q f_q \mathbf{c}_{k-q}, \quad \eta^\dagger \mathbf{c}_k^\dagger \eta = \sum_q f_q^* \mathbf{c}_{k-q}^\dagger. \quad (3.7)$$

where we introduced the Fourier components of  $e^{i\varphi(x)}$  by

$$e^{i\varphi(x)} = f(x) = \sum_{q \in \text{Bz}} f_q e^{iqx}, \quad (3.8)$$

with  $q = 2\pi n_q/N$  ( $n_q \in \mathbb{N}$ ) and

$$\begin{aligned} f_q &= 2 \frac{1 - e^{-i\pi n_q}}{1 - e^{-i2\pi n_q/N}} \\ &= \begin{cases} \frac{4}{1 - e^{-i2\pi n_q/N}}, & n_q = 1, 3, \dots, N-1, \\ 0, & n_q = 0, 2, \dots, N-2. \end{cases} \end{aligned} \quad (3.9)$$

In a basis that diagonalizes the Hamiltonian,

$$\eta^\dagger \boldsymbol{\alpha}_k \eta = \sum_{k'} \mathbf{S}_{k,k'}^\dagger \boldsymbol{\alpha}_{k'}, \quad \eta^\dagger \boldsymbol{\alpha}_k^\dagger \eta = \sum_{k'} \boldsymbol{\alpha}_{k'}^\dagger \mathbf{S}_{k,k'} (3.10)$$

where a  $2N \times 2N$  matrix  $\mathbf{S}_{(k\iota)(k'\lambda)}$  is given by

$$\mathbf{S}_{(k\iota)(k'\lambda)} = \sum_q f_q^* [v^\dagger(k-q)v(k)]_{\iota\lambda} \delta_{k-q,k'}, \quad (3.11)$$

and  $v^\dagger(p) = (v_+^\dagger(p), v_-^\dagger(p))$ .

The expectation value of the kink operator with respect to  $|\Psi\rangle$  is then represented as the determinant of  $N \times N$  matrix  $\mathbf{S}_{(k-)(k'-)}$ ,

$$\langle \Psi | \eta | \Psi \rangle = \det [\mathbf{S}_{(k-)(k'-)}]. \quad (3.12)$$

If we define the “hopping” elements  $t_{p,q}$  through

$$t_{k,k-q} := [v^\dagger(k)v(k-q)]_{--}, \quad (3.13)$$

the matrix  $\mathbf{S}_{(k-)(k'-)}$  in Eq. (3.12) can be represented by a tight-binding Hamiltonian as,

$$\begin{aligned} \mathcal{S} &= \sum_{k,k'} a_k^\dagger \mathbf{S}_{(k-)(k'-)} a_{k'} \\ &= \sum_k \sum_q f_q t_{k,k-q} a_k^\dagger a_{k-q}. \end{aligned} \quad (3.14)$$

where  $a_p^\dagger/a_p$  represents fermionic creation/annihilation operator defined for  $p \in \text{Bz}$ . This Hamiltonian can be interpreted as describing a quantum particle hopping on a 1D lattice. Note that the gauge field  $A_x(k)$  and the metric  $g_{xx}(k)$  are related to the phase and the amplitude of the nearest neighbour hopping elements  $t_{k,k-2\pi/N}$ , respectively. The hopping matrix  $t_{k,k-q}$  is generically non-local. Also, since the kink operator introduces a sharp boundary in the real space, the dual Hamiltonian is highly non-local in  $k$ -space.

It is evident from Eq. (3.12) that the vanishing of  $\langle \Psi | \eta | \Psi \rangle$  is equivalent to existence of zero modes in the spectrum of the  $\mathcal{S}$ -Hamiltonian. As we will see below, the spectrum of the  $\mathcal{S}$ -Hamiltonian is pretty much similar to that of the  $\mathcal{C}$ -Hamiltonian: away from a critical point, the spectrum is gapped and all the eigenvalues are close to either  $+1$  or  $-1$ , except a few eigen values in the gap that reflect the Berry phase if it is non-trivial. If the Berry phase is  $\pi \times$  odd integer, there are exact zero energy eigen modes. When we approach a critical point, eigenvalues proliferate around zero energy. Roughly speaking, the entanglement entropy takes into account the distribution of *all* the eigenvalues of  $\mathcal{S}$ , whereas the kink operator only takes into account the products of all the eigenvalues.

### B. “chiral symmetry” and “time-reversal symmetry”

The  $\mathcal{S}$ -Hamiltonian has a chiral symmetry, which directly reflects our bipartitioning the original system and has nothing to do with the chiral symmetry in the original system. Indeed, from Eq. (3.9), one can see that  $a_k$  with  $k$  odd/even are connected to  $a_{k'}$  with  $k'$  odd/even only. All the eigen states in  $k$ -space are connected to their partner with the opposite energy via

$$a_k \rightarrow a'_k = (-1)^{i\pi n_k} a_k, \quad k = \frac{2\pi n_k}{N}. \quad (3.15)$$

which in turn means in the real space

$$a_x \rightarrow a_{x+N_A} = a'_x. \quad (3.16)$$

When the original system respects the chiral symmetry (not to be confused with the chiral symmetry above), all the single particle wave function  $\psi(k)$  of  $\mathcal{S}$  in  $k$ -space can be taken to be real by a suitable rotation in  $\mathbf{R}$ -space. [However when the Berry phase is  $\gamma = \pi \times$  integer, this comes with a price to have a Dirac string that intersect  $\mathbf{R}(k)$ .] The ability of taking all “hopping” elements  $t_{k,k'}$  to be real induces an additional “time-reversal symmetry” to  $\mathcal{S}$ -Hamiltonian; the phase associated with  $f_q$  can be removed by a simple gauge transformation,

$$a_k \rightarrow b_k = e^{+ik/2 - ikN_A/2} a_k. \quad (3.17)$$

[See Fig. 3.] Thus, we can take all the matrix elements  $f_q t_{k,k-q}$  in the  $\mathcal{S}$ -Hamiltonian to be real. Furthermore, when we go back to the real space, this “time-reversal” invariance implies a parity symmetry with respect to an inversion center  $x_0 = -N_A/2 + 1/2$ . To see this, we first note that all the one-particle eigen states of  $\mathcal{S}$  can be taken real in the basis  $\{b_p^\dagger, b_p\}$ ; the  $\mathcal{S}$ -Hamiltonian can be diagonalized as  $\mathcal{S} = \sum_n \epsilon_n d_n^\dagger d_n$  with

$$b_p = \sum_n \phi_n(p) d_n, \quad b_p^\dagger = \sum_n \phi_n(p) d_n^\dagger, \quad (3.18)$$

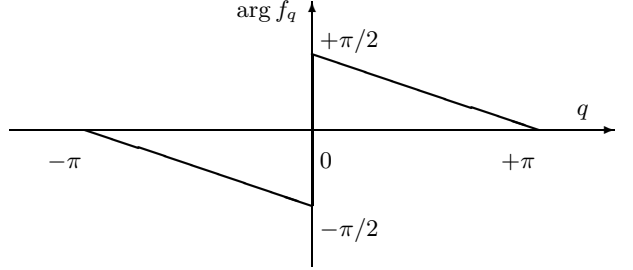


FIG. 3:  $\arg f_q = \arg \left( 4 \frac{1}{1 - e^{-iq}} \right) = -\arg (1 - e^{-iq})$  for  $n_q = 1, 3, 5, \dots, N-1$ .

where  $\phi_n(p)$  is a eigen wavefunction which is real. Since the basis  $\{a_x^\dagger, a_x\}$  and  $\{d_n^\dagger, d_n\}$  are related through

$$a_x = \sum_n \frac{1}{\sqrt{N}} \sum_k e^{ik(x-1/2+N_A/2)} \phi_n(k) d_n, \quad (3.19)$$

the real space eigen wavefunctions  $\psi_n(x)$  in the basis  $\{a_x^\dagger, a_x\}$  are given by

$$\psi_n(x) = \frac{1}{\sqrt{N}} \sum_k e^{ik(x-1/2+N_A/2)} \phi_n(k), \quad (3.20)$$

from which one can see  $\psi_n(x)$  satisfies

$$[\psi_n(x)]^* = \psi_n(-x + 1 - N_A). \quad (3.21)$$

I.e., the wave function amplitude is parity symmetric with respect to  $x_0 = -N_A/2 + 1/2$ .

This time-reversal symmetry, which is a reincarnation of the chiral symmetry of the Hamiltonian  $\mathcal{H}$ , plays an important role for the vanishing of the expectation value of the kink operator. Indeed, it is this symmetry which guarantees existence of zero-modes of  $\mathcal{S}$ .

### C. the existence of zero-modes

The argument that tells us the existence of zero modes for the  $\mathcal{S}$ -Hamiltonian is somewhat similar to the “proof” of the existence of zero modes for the  $\mathcal{C}$ -Hamiltonian in that we consider a adiabatic change of the Hamiltonian. The major difference comes from the fact that the chiral symmetry in the  $\mathcal{S}$ -Hamiltonian is implemented as a kind of time-reversal symmetry as we discussed before.

We first establish that there is a pair of zero modes for  $\mathcal{S}$  when we take  $|\Psi\rangle$  as the ground state of the dimerized Hamiltonian (2.11) with the chiral symmetry. The hopping elements in  $\mathcal{S}$  are computed from the overlap of the Bloch wave functions as

$$\begin{aligned} & \langle v_\pm(p) | v_\pm(q) \rangle \\ &= \frac{1}{2R(R \mp R^3)} \left[ \Delta^2 e^{i(p-q)} + R^2 \mp 2R\xi + \xi^2 \right]. \end{aligned} \quad (3.22)$$

The  $\mathcal{S}$ -Hamiltonian is then diagonalized as

$$\begin{aligned} \mathcal{S} &= \frac{1}{2R(R - R^3)} \\ &\times \sum_x \left[ \Delta^2 f(x+1) + (R - \xi)^2 f(x) \right] a_x^\dagger a_x. \end{aligned} \quad (3.23)$$

We see that there are two mid-gap states with energies  $\pm \xi/R$ . Especially when  $\xi = 0$ , there are a pair of zero energy states localized at the interfaces.

We then change the Hamiltonian in a continuous fashion in such a way that (i) it respects the chiral symmetry during the deformation, and (ii) it does not cross the gap closing point (the origin of  $\mathbf{R}$ -space). During this deformation, the Berry phase of the ground state wavefunction is always kept to be  $\pi$ . As already discussed, we can take all the Bloch wave functions to be real and there is a “time-reversal” symmetry.

One can see that the zero modes never escape from  $E = 0$  as it constrained by the time-reversal symmetry, which is nothing but the parity invariance with respect to  $x_0 = -N_A/2 + 1/2$ . First note that since the  $\mathcal{S}$ -Hamiltonian in  $k$ -space is non-local, it is short-ranged (quasi-diagonal) in the real space. Thus, if we take the thermodynamic limit  $N \rightarrow \infty$ , states that appear between the gap are spatially localized near the interfaces located  $x = 1/2$  and  $x = N_A + 1/2$ , which separate the system into the two subsystems.

During the deformation, the two localized states, which located at  $x = 1/2$  and  $x = N_A + 1/2$ , respectively, can in principle go away from  $E = 0$ . Due to the “chiral symmetry” of the  $\mathcal{S}$ -Hamiltonian, if one goes up from  $E = 0$ , the other must be go down. However, if there is the “time-reversal symmetry”, each eigenstate must be invariant under the space inversion with respect to  $-N_A/2 + 1/2$ . In order for the localized states to satisfy these two conditions, both of them must be located at  $E = 0$ .

As an example, the spectrum of the  $\mathcal{S}$ -Hamiltonian for the SSH model is presented in Fig. 2. The spectrum is almost identical to that of the  $\mathcal{C}$ -Hamiltonian and a pair of zero modes persists for the entire quantum phase  $\phi \in [-1, 0]$ .

#### IV. 2D SYSTEMS WITH THE NON-VANISHING CHERN NUMBER

As far as we consider translational invariant systems, the above 1D discussions still apply to higher dimensions. When a  $d$ -dimensional translational invariant system is bipartitioned by a  $(d-1)$ -dimensional hyperplane, we can perform the  $(d-1)$ -dimensional Fourier transformation along the interface. The Hamiltonian is block-diagonal in terms of the wave number along the interface  $\mathbf{k}$ ,  $\mathcal{H} = \sum_{\mathbf{k}} \mathcal{H}(\mathbf{k})$ , where  $\mathcal{H}(\mathbf{k})$  is a 1D Hamiltonian for each  $\mathbf{k}$ -subspace. Then, the previous discussion applies to each  $\mathcal{H}(\mathbf{k})$ . As an example of a 2D two-band system, let us

consider 2D chiral  $p$ -wave superconductor ( $p$ -wave SC) defined by

$$\begin{aligned} \mathcal{H} &= \sum_{\mathbf{r}} \mathbf{c}_{\mathbf{r}}^\dagger \begin{pmatrix} t & \Delta \\ -\Delta & -t \end{pmatrix} \mathbf{c}_{\mathbf{r}+\hat{\mathbf{x}}} + \text{h.c.} \\ &+ \mathbf{c}_{\mathbf{r}}^\dagger \begin{pmatrix} t & i\Delta \\ i\Delta & -t \end{pmatrix} \mathbf{c}_{\mathbf{r}+\hat{\mathbf{y}}} + \text{h.c.} + \mathbf{c}_{\mathbf{r}}^\dagger \begin{pmatrix} \mu & 0 \\ 0 & -\mu \end{pmatrix} \mathbf{c}_{\mathbf{r}}, \end{aligned} \quad (4.1)$$

where the index  $\mathbf{r}$  runs over the 2D square lattice and  $t, \Delta, \mu \in \mathbb{R}$ . For simplicity, we set  $t = \Delta = 1$  in the following. The chiral  $p$ -wave SC has been discussed in the context of super conductivity in a ruthenate and paired states in the fractional quantum Hall effect. [29, 30, 31, 32, 33, 34] There are four phases separated by three quantum critical points at  $\mu = 0, \pm 4$ , which are labeled by the Chern number  $Ch$  as  $Ch = 0$  ( $|\mu| > 4$ ),  $Ch = -1$  ( $-4 < \mu < 0$ ), and  $Ch = +1$  ( $0 < \mu < +4$ ). The non-zero Chern number implies the IQHE in the spin transport. [31]

The energy spectrum of the family of Hamiltonians  $\mathcal{H}(k_y)$  parametrized by the wave number in  $y$ -direction,  $k_y$ , is given in Fig. 4. There are branches of edge states that connects the upper and lower band for phases with  $Ch = \pm 1$ . These edge states contributes to the entanglement entropy. The energy spectrum of the  $\mathcal{C}$ -Hamiltonian with open ends is shown in Fig. 4. The corresponding entanglement entropy is also found in Fig. 4. Since there are contributions from the edge states, cusp structures are seen in the entanglement entropy.

The band structure at the critical points  $\mu = \pm 4$  consists of one gapless Dirac fermion. It can be interesting to ask how much entanglement entropy is carried by a Dirac fermion since it is just in-between of a fully gapped system and a system with a finite Fermi surface; for the former the entanglement entropy satisfies the area law, whereas for the latter there is a log-correction to the area law. [28] Unlike the case of a finite Fermi surface, the entanglement entropy divided by  $N_y$ ,  $S_A/N_y$  is constant for a system with Dirac fermions; The energy spectrum close to a gap closing point  $\mathbf{k}^{(0)}$  is linear and so is the mass gap as a function of  $k_y$ ,  $m(k_y) \propto k_y - k_y^{(0)}$ . Combining this fact with the known result for a massive 1D system, each  $k_y$  contributes to the entanglement entropy by  $\sim \frac{1}{6} \ln m(k_y)^{-1}$ . Integrating these contributions around  $k_y^{(0)}$  we see that the entanglement entropy behaves as  $S_A \sim \alpha N_y$ . Adding the contribution just at the gap closing point, we thus obtain  $S_A \sim \alpha N_y + \beta \ln N_y - \gamma + \dots$  for a single Dirac fermion where  $\alpha, \beta, \gamma$  is some constant. Hence  $S_A/N_y$  is finite. For fully gapped topological field theories (i.e.,  $\beta = 0$ ), the  $N_y$ -independent piece of  $S_A$ ,  $-\gamma$  (should not be confused with the Berry phase), is shown to be universal and called the topological entropy in [35, 36].

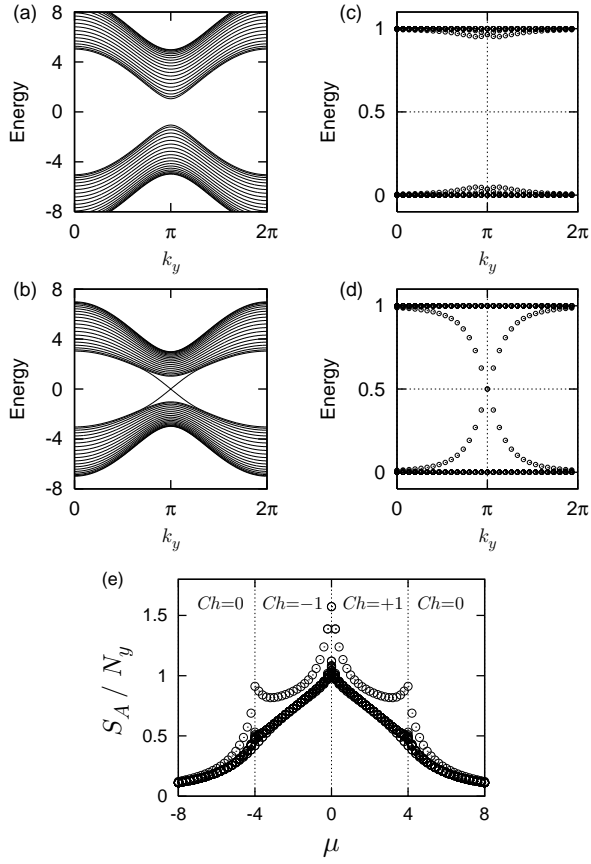


FIG. 4: The energy spectrum v.s.  $k_y \in [0, 2\pi]$  for the 2D  $p$ -wave SC with boundaries. The chemical potential is  $\mu = -5$  (a) and  $-3$  (b) and  $t = \Delta = 1$ . The corresponding spectra of the  $\mathcal{C}$ -Hamiltonian are shown in (c) ( $\mu = -5$ ) and (d) ( $\mu = -3$ ). The entanglement entropy of the 2D chiral  $p$ -wave SC as a function of  $\mu$  is presented in (e). The aspect ratio  $r = N_y/N_x$  is  $r = 1/2, 1/3, 1/4, 1/8$  from the bottom at  $\mu = -4$ .

## V. CONCLUSION

We have identified two types of contributions to the entanglement entropy, i.e., one from the boundaries of the system created by taking the partial trace and the other from the bulk energy spectrum. The contribution from the boundaries is controlled by the Berry phase and hence we can make use of some known facts on the “bulk-boundary correspondence” to compute the entanglement entropy. Especially, we have obtained the lower bound of the entanglement entropy for 1D systems with discrete particle-hole symmetries.

An interesting and direct application of the present result is the entanglement entropy of 2D  $d$ -wave superconductors and carbon nanotubes. In these systems, different ways of bipartitioning the system lead to different amounts of the entanglement entropy. [18]

Extensions to multi-band systems, especially to the case of completely degenerate bands might be also in-

teresting in which we need to use the non-Abelian Berry phase to characterize the system. [37] A more fundamental question is that how one can characterize, with the entanglement entropy of several types, several spin liquid states in higher dimensions (including gapless systems) with several quantum orders.

## Acknowledgments

We are grateful to R. Shindou for useful discussions. This research was supported in part by the National Science Foundation under Grant No. PHY99-07949 (SR) and a Grant-in-Aid from the ministry of Education, Culture, Sports, Science and Technology, Japan (YH).

## APPENDIX A: THE DUAL BERRY PHASE

In this appendix, we introduce the dual Berry phase  $\bar{\gamma}$  in the 1D two-band Hamiltonian Eq. (2.1). It is in spirit similar to the dual order parameter (disorder parameter) in the Ising spin chain; if we impose the chiral symmetry, in a quantum phase with  $\gamma = 0$  the dual Berry phase is given by  $\bar{\gamma} = -\pi$  whereas when  $\gamma = -\pi$ ,  $\bar{\gamma} = 0$ . Thus a quantum phase is characterized by both  $\gamma$  and  $\bar{\gamma}$ .

Let us first introduce dimer operators by

$$d_{\pm, x+\frac{1}{2}}^\dagger = \frac{1}{\sqrt{2}} (c_{+, x}^\dagger \pm c_{-, x+1}^\dagger). \quad (\text{A1})$$

When written in terms of the dimer operators, the Hamiltonian reads  $\mathcal{H} = \frac{1}{2} \sum_{x, x'}^{\text{PBC}} \mathbf{d}_{x+\frac{1}{2}}^\dagger \bar{H}_{x-x'} \mathbf{d}_{x'+\frac{1}{2}}^\dagger$ , where the new hopping matrix elements  $\bar{H}_{x-x'}$  are some function of the original ones  $H_{x-x'}$ . For simplicity, we focus on the case of particle-hole symmetric ( $t_+ = -t_-$ ) and translational invariant systems. In the momentum space, the Hamiltonian is given by  $\mathcal{H} = \sum_{k \in \text{Bz}} \mathbf{d}_k^\dagger \bar{\mathbf{R}}(k) \cdot \boldsymbol{\sigma} \mathbf{d}_k$  with a 3D vector  $\bar{\mathbf{R}}(k)$  given by

$$\begin{aligned} \bar{R}_x(k) &= R_z(k), \\ \bar{R}_y(k) &= \sin(k)R_x(k) + \cos(k)R_y(k), \\ \bar{R}_z(k) &= \cos(k)R_x(k) - \sin(k)R_y(k). \end{aligned} \quad (\text{A2})$$

We define the dual Berry phase  $\bar{\gamma}$  as the Berry phase for the dual 3D vector  $\bar{\mathbf{R}}(k)$ ,

$$\bar{\gamma} := \int_0^{2\pi} dk \langle \bar{v}(k) | \frac{d}{dk} | \bar{v}(k) \rangle = \int_0^{2\pi} dk \frac{\bar{X} \dot{\bar{Y}} - \bar{Y} \dot{\bar{X}}}{2\bar{R}(\bar{R} - \bar{Z})}. \quad (\text{A3})$$

where  $\dot{X} = dR_x(k)/dk$ , etc. Rotating  $\bar{\mathbf{R}}$  around  $\bar{R}_y$ -axis as  $(\bar{R}_x, \bar{R}_y, \bar{R}_z) \rightarrow (\bar{R}_z, \bar{R}_y, -\bar{R}_x)$ , and noting  $\bar{Y} \dot{\bar{X}} - \bar{X} \dot{\bar{Y}} = X \dot{Y} - Y \dot{X} + X^2 + Y^2$ , the dual Berry phase is thus given by

$$\bar{\gamma} = -\gamma - \pi - \int_0^{2\pi} dk \frac{Z}{2R} \quad (\text{A4})$$

Especially if we impose the chiral symmetry,  $\mathbf{R}$  is restricted to  $XY$ -plane and thus

$$\bar{\gamma} = -\gamma - \pi. \quad (\text{A5})$$

---

[1] X. G. Wen, Phys. Rev. B **40**, 7387 (1989); X. G. Wen and Q. Niu, Phys. Rev. B **41**, 9377 (1990); X. G. Wen, “Quantum Field Theory of Many-Body Systems”, Oxford University Press, (2004).

[2] The base of logarithm can be taken either  $e$  or 2, depending on literatures.

[3] C. Holzhey, F. Larsen, and F. Wilczek, Nucl. Phys. B **424**, 443 (1994).

[4] A. Osterloh, L. Amico, G. Falci, and R. Fazio, Nature, **416**, 608 (2002).

[5] T. J. Osborne and M. A. Nielsen, Phys. Rev. A **66**, 032110 (2002).

[6] G. Vidal, J. I. Latorre, E. Rico and A. Kitaev, Phys. Rev. Lett. **90**, 227902 (2003).

[7] H. Fan, V. Korepin and V. Roychowdhury, Phys. Rev. Lett. **93**, 227203 (2004).

[8] P. Calabrese, and J. Cardy, [hep-th/0405152](#).

[9] S. Furukawa, G. Misguich, and M. Oshikawa, [cond-mat/0508469](#).

[10] M. V. Berry, Proc. R. Soc. **A392**, 45 (1984).

[11] D. J. Thouless, M. Kohmoto, P. Nightingale, and M. den Nijs, Phys. Rev. Lett. **49**, 405 (1982).

[12] M. Kohmoto, Ann. Phys. (N.Y.) **160** 355 (1985).

[13] J. Zak, Phys. Rev. Lett. **62**, 2747 (1989).

[14] R. D. King Smith and D. H. Vanderbilt, Phys. Rev. B. **47**, 1651 (1993); Phys. Rev. B. **48**, 4442 (1993).

[15] R. Resta, Rev. Mod. Phys. **66**, 899 (1994).

[16] M. den Nijs and K. Rommelse, Phys. Rev. B. **40**, 4709 (1989).

[17] M. Nakamura and S. Todo, Phys. Rev. Lett. **89**, 077204 (2002).

[18] S. Ryu and Y. Hatsugai, Phys. Rev. Lett. **89**, 077002 (2002).

[19] Y. Hatsugai, Phys. Rev. Lett. **71**, 3697 (1993).

[20] A. Y. Kitaev, [cond-mat/0010440](#).

[21] N. Marzari, and D. Vanderbilt, Phys. Rev. B **56**, 12847 (1997).

[22] S. Onoda, S. Murakami, and N. Nagaosa, Phys. Rev. Lett. **93**, 167602 (2004).

[23] The expectation value of the twist operator (Eq. (2.5)) can be obtained in a similar fashion to that of the kink operator, see Sec. III A.

[24] I. Peschel, [cond-mat/0212631](#).

[25] The similar criterion can be developed for systems with Kramers degeneracy. There, the time-reversal symmetry can be used as the 2nd particle-hole symmetry in addition to the chiral symmetry. [18]

[26] A. Heeger, S. Kivelson, J. R. Schrieffer, and W. -P. Su, Rev. Mod. Phys. **60**, 781 (1988).

[27] R. Shindou, K. Imura, M. Ogata, unpublished.

[28] M. M. Wolf, [quant-ph/0503219](#).

[29] N. Read and D. Green, Phys. Rev. B **61**, 10267 (2000).

[30] G. E. Volovik, Pis'ma ZhETF, JETP Lett. **66**, 493 (1997).

[31] T. Senthil, M. P. A. Fisher, L. Balents and C. Nayak, Phys. Rev. Lett. **81**, 4704 (1998).

[32] J. Goryo and K. Ishikawa, Phys. Lett. A **260**, 294 (1999).

[33] Y. Morita and Y. Hatsugai, Phys. Rev. B **62**, 99 (2000).

[34] Y. Hatsugai and S. Ryu, Phys. Rev. B **65**, 212510 (2002).

[35] A. Kitaev, and J. Preskill, [hep-th/0510092](#).

[36] M. Levin and X. G. Wen, [cond-mat/0510613](#).

[37] Y. Hatsugai, J. Phys. Soc. Jpn. **73** 2604 (2004); J. Phys. Soc. Jpn. **74** 1374 (2005).